



Removal of Pb (II) from aqueous solution using nanoadsorbent of *Oryza sativa* husk: Isotherm, kinetic and thermodynamic studies



Mandeep Kaur^{a,*}, Santosh Kumari^b, Praveen Sharma^a

^a Department of Environmental Science & Engineering, Guru Jambheshwar University of Science & Technology, Hisar 125001, Haryana, India

^b Department of Bio & Nano Technology, Guru Jambheshwar University of Science & Technology, Hisar 125001, Haryana, India

ARTICLE INFO

Article history:

Received 2 August 2019

Received in revised form 3 December 2019

Accepted 3 December 2019

Keywords:

Nanoadsorbent
Oryza sativa husk
Adsorption
Lead
Equilibrium
Kinetics

ABSTRACT

This research focus on the removal of Pb (II) ions from aqueous solution by adsorption process using nanoadsorbent developed from agricultural waste *Oryza sativa* husk (OSH). Surface morphology of nanoadsorbent was analyzed by FE-SEM, elemental composition by EDX and size by AFM. Attachment of functional groups on nanoadsorbent was determined by FTIR. The effect of pH, dose, contact time, initial concentration and temperature were investigated. Optimum adsorption of lead at pH 8, contact time 70 min at 60 °C temperature with 0.6 g/50 mL nanoadsorbent dose obeyed pseudo second order kinetic model with R^2 0.996. Pb (II) adsorption was analyzed by Freundlich, Langmuir and Temkin models. Freundlich isotherm model with correlation coefficient R^2 0.999 was best fitted. Thermodynamic parameters anticipated the adsorption process to be endothermic and spontaneous. Post adsorption elution was carried out successfully. Results demonstrate that OSH is a low cost and eco-friendly choice for Pb (II) remediation.

© 2019 Published by Elsevier B.V. This is an open access article under the CC BY-NC-ND license (<http://creativecommons.org/licenses/by-nc-nd/4.0/>).

1. Introduction

Indefinite persistence of organic/inorganic pollutants (heavy metals) causes pollution of air, soil and water that seems to be the major environmental concerns [1,2]. Non-biodegradable pollutants i.e. heavy metals can bioaccumulate in the living organisms via food chain, drinking water and air [3] and getting dangerous for human beings, aquatic life and ultimately the ecosystem [4]. Water the most precious natural resource is getting affected by industrial discharge of chemicals mainly heavy metals [5]. Among several heavy metals viz. lead, zinc, copper, cadmium, arsenic, chromium etc. lead is the grievous one due to its acute toxicity. Otherwise lead is considered to be useful in water distribution system which contains lead pipes or lead solders and in manufacturing products like paints, cosmetics, ceramic glazes, crystal glassware etc. Highly poisonous and non-biodegradable lead can cause renal disorders, destroy RBCs, damage central nervous system and ultimately death [6,7]. Prenatal lead exposure is associated with adverse effects of maternal depression, gestational hypertension, low birth weight and spontaneous abortion [8]. Emission of lead from various industrial activities in mining, smelting, power plants, gasoline, incinerators, plumbing and households and currently chronic

toxicity of lead from generation of e-wastes tends to result in severe health hazards [9]. Such heavy metals need to be addressed and polished off.

To decelerate the trouble caused by heavy metal contamination in the environment, different treatment technologies viz. chemical precipitation [10], electrolysis, ion exchange [11], membrane filtration [12] and reverse osmosis [13] have been adopted by different researchers. These conventional technologies have certain drawbacks such as toxic chemical sludge production in excess, increased sludge production cost, high equipment cost, high energy consumption, low purification efficiency in industrial applications and non-ecofriendliness [14]. However, adsorption is more focused and outmatching in terms of low economic cost, high efficiency, regeneration efficiency and environment friendly approach also reported by [15,16]. Adsorption occurs due to physico-chemical interchanges of metal ions with different functional groups viz. phosphate, sulphate, amino, carboxylic and hydroxyl groups. Recently nanomaterials especially nanocellulose extracted from sustainable agricultural wastes because of its exceptional properties viz. high surface area, greater metal binding sites and high regeneration efficiency has been widely studied as adsorbent to eliminate metal ions from synthetic solution [17]. In present research work, agricultural waste-*Oryza sativa* husk (OSH) which is a nuisance to the environment (due to hazardous practice of stubble burning resulting into immense air pollution rampantly) has been prominently harnessed to develop nanocellulose by chemo-mechanical method. Nanocellulose has

* Corresponding author.

E-mail addresses: mandeepkaur76@gmail.com (M. Kaur), kaushdbs@gmail.com (S. Kumari), praveen.gju@gmail.com (P. Sharma).

significant features like biodegradability, renewability, large surface area and greater strength [18]. The novel product nanocellulose is further used as nanoadsorbent OSH for binding lead metal and subsequent removal of lead from contaminated aqueous channel.

2. Materials and methods

2.1. Materials

AR grade chemicals were used. Lead nitrate was supplied by TM media Pvt. Ltd., India. SD Fine Chem. Ltd., Mumbai supplied NaOH (pellets) and H₂SO₄. NaClO₂ was obtained from CDH.

2.2. Methods

2.2.1. Preparation and characterization of nanocellulose

Nanocellulose was prepared from agricultural waste material *Oryza sativa* husk (OSH) as reported earlier [19]. *Oryza sativa* husk (OSH) was gathered from nearby agricultural store. It was soaked in water and washed to cut down impurities, completely ground, sieved and brought up for chemo-mechanical treatment. Sequence of treatment steps followed were (i) alkali treatment, (ii) bleaching treatment (iii) acid hydrolysis (iv) centrifugation, (v) ultrasonication and (vi) magnetic stirring as reported earlier [1]. The homogenized mixture (nanocellulose) obtained was further characterized by employing different techniques. The size of nanocellulose was observed by Atomic Force Microscopy. Surface morphology before and after lead adsorption was analyzed by Field-Emission Scanning Electron Microscopy and Energy Dispersive X-ray spectroscopy was applied to find out elemental composition. Attachment of functional groups on the nano-adsorbent surface was identified by Fourier Transform Infrared spectrum using KBr pellets with 400–4000 cm⁻¹ wavelength range. The quantification of metal ion concentration in the solution was observed by AAS (Atomic Absorption Spectrophotometer). The characterized nanocellulose was further used as nanoadsorbent for Pb (II) removal.

2.3. Batch adsorption experiments

Lead nitrate was used to prepare 1000 mg/L Pb (II) standard stock solution. Thereafter dilution for the solution was made upto required concentrations for further use in the experiments. pH of

the solution was maintained by HCl and NaOH (0.1 M). Adsorption of Pb (II) onto nanocellulose (used as nanoadsorbent) was studied in batch mode. The metal removal study was carried out with 50 ml aqueous solution of respective metal (10–100 mg/L known concentration) by mixing 0.6 g adsorbent dose for 90 min at 180 rpm at 27 ± 1 °C temperature. The mixture was filtered and residual lead concentration was found out. The efficiency for lead removal (% R) and equilibrium adsorption capacity of lead (q_e) were estimated by the Eqs. (1) & (2):

$$\text{Removal of metal (\% R)} = \frac{C_i - C_e}{C_e} \times 100 \quad (1)$$

$$\text{Equilibrium adsorption capacity (q}_e\text{)} = \frac{(C_i - C_e) V}{M} \quad (2)$$

Where C_i initial and C_e final lead concentration (mg/L), q_e (mg/g) metal amount adsorbed on the adsorbent at equilibrium, V (L) metal ion solution volume and M (g) mass of the adsorbent.

3. Results and discussion

3.1. Characterization

Three-dimensional image of the synthesized nanocellulose in Fig. 1 shows spherical particles on rough surface due to aggregation after acid hydrolysis with sulphuric acid. The diameter range of nanocellulose was 50–100 nm with some of the round patches having 76.77 nm diameter. Similar trend was described by [20]. Surface morphology prior to deposition of lead ions and after deposition of lead ions onto the surface of nanocellulose was substantiated by field-emission scanning electron microscopy (FE-SEM). The irregular broken fibres of nanocellulose after hydrolysis with 100 μm diameter are clearly visible in Fig. 2 and after adsorption there are bright agglomerations of lead ions on the nanoadsorbent of diameter 10 μm as shown in Fig. 3. Elemental composition of lead loaded nanoadsorbent exhibited in Fig. 4 is weight percent of carbon (44.22 %), oxygen (44.20 %), lead (6.06 %), Si (0.39 %) and Au (5.13 %) corroborating to their binding energies. FTIR spectrum of nanocellulose with adhered functional groups is presented in Fig. 5. The peak in the region 3400–3440 cm⁻¹ is imputed O–H group stretching. The peak at 2924 cm⁻¹ corresponds to C–H stretching vibration of methylene group. The absorption peak near 1635–1651 cm⁻¹ is assigned to O–H turning

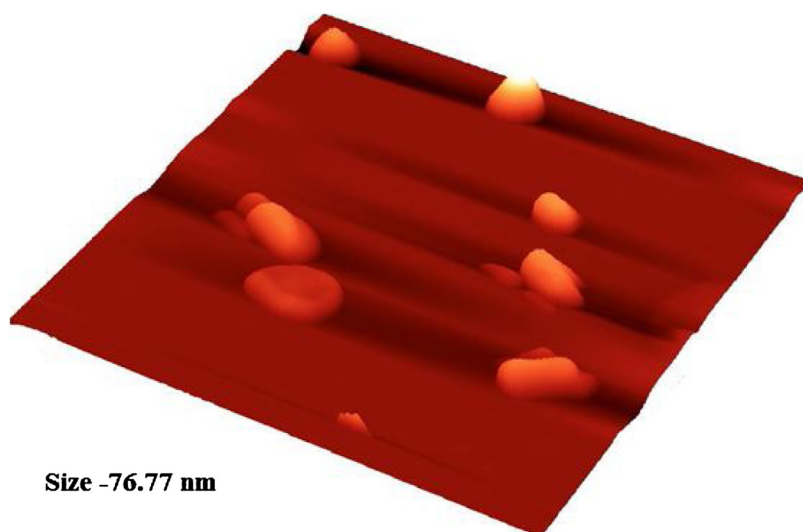


Fig. 1. AFM image of nanocellulose synthesized from *Oryza sativa* husk.

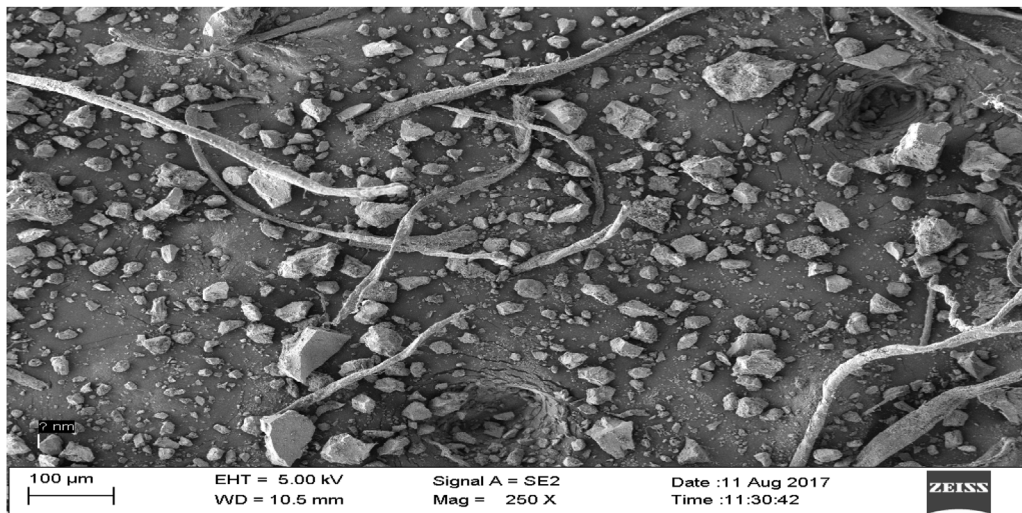


Fig. 2. (a) FESEM image of nanocellulose synthesized from *Oryza sativa* husk.

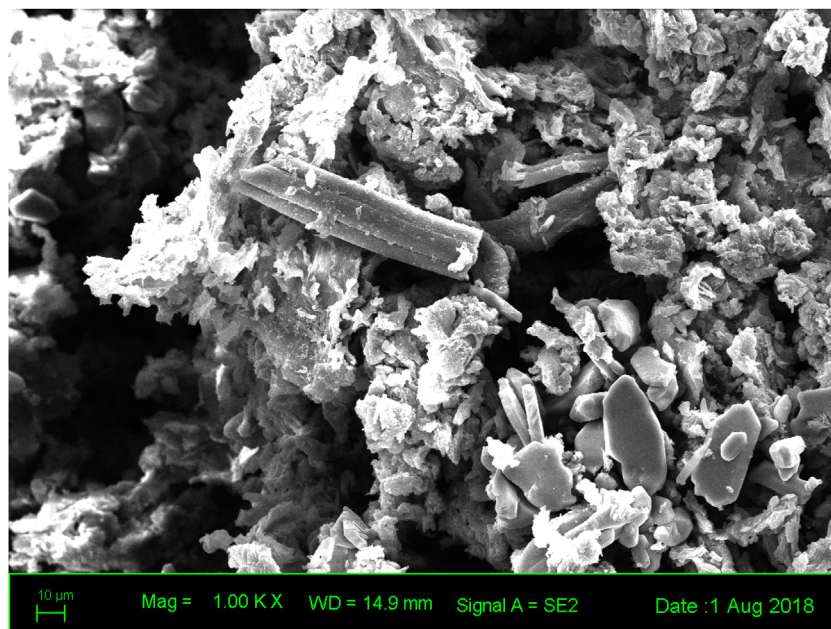


Fig. 3. FESEM image of lead loaded nanocellulose synthesized from *Oryza sativa* husk.

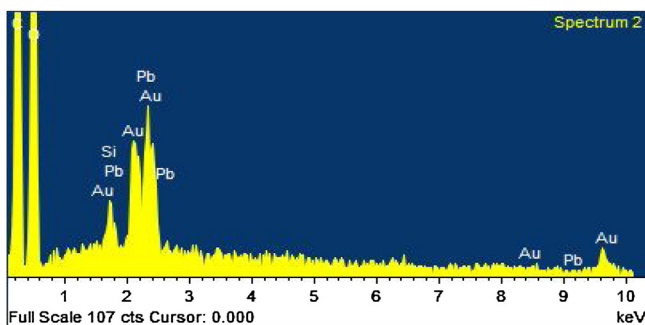


Fig. 4. EDX spectrum of lead loaded nanocellulose synthesized from *Oryza sativa* husk.

of water adsorbed and in the region $1155\text{--}1160\text{ cm}^{-1}$ peaks are ascribed to glycosidic ether linkage C--O--C and C--C ring stretching respectively. The corresponding at 1024 cm^{-1} and 896 cm^{-1} are due to C--O--C stretching vibration of glycosidic

linkage between glucose units in cellulose and pyranose ring suggested by [19].

3.2. Batch adsorption studies

3.2.1. Effect of pH on Pb (II) removal

Speciation properties of metal, charge on the adsorbent surface and ionization degree are the factors greatly affected by pH relative to adsorption mechanism and uptake capacity of the lead ions [21,22]. pH effect on the removal of Pb (II) by proposed nanoadsorbent is presented in Fig. 6 which indicate gradual rise in removal of lead i.e. 77%–87% when pH was varied from 2–8. Due to greater strengthening of protons, active binding sites on adsorbent surface get protonated at low pH, consequently binding of metal ions get reduced [38]. The positively charged functional groups may not associate for binding of metal ions. Whereas at pH 8, the surface of nanoadsorbent becomes negatively charged due to ionization of functional groups OH^- and COO^- of nanocellulose and exchange of ions takes place between the functional groups

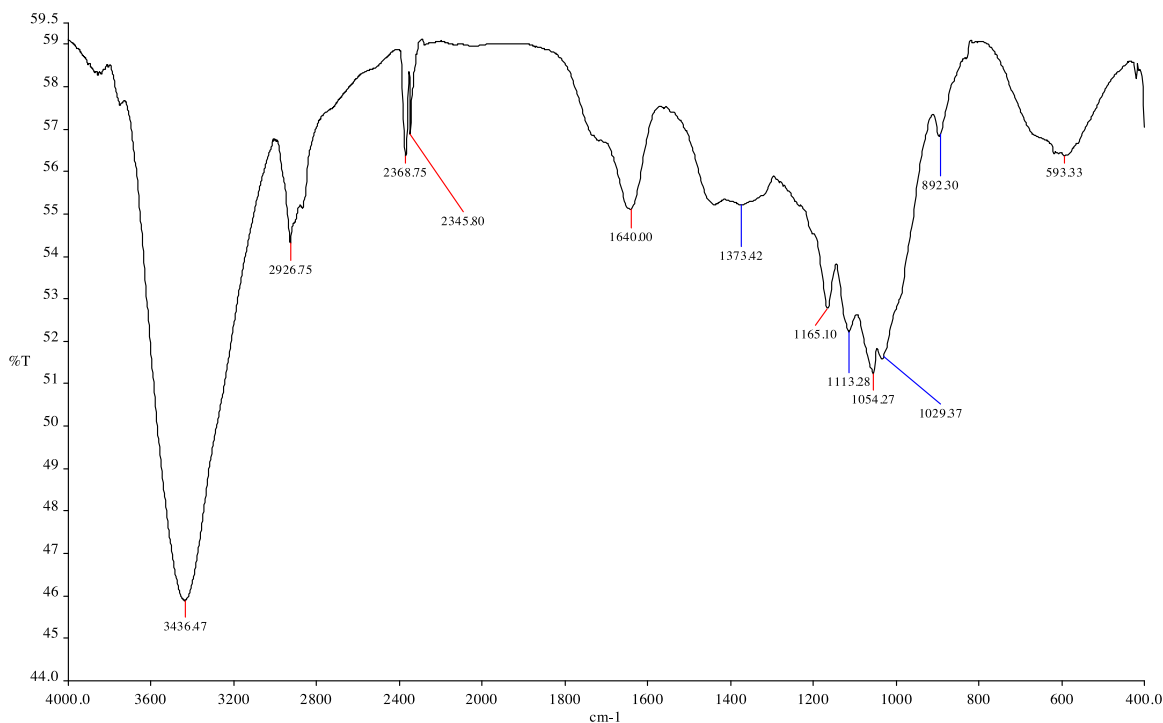


Fig. 5. FTIR spectra of acid hydrolysed *Oryza sativa* husk.

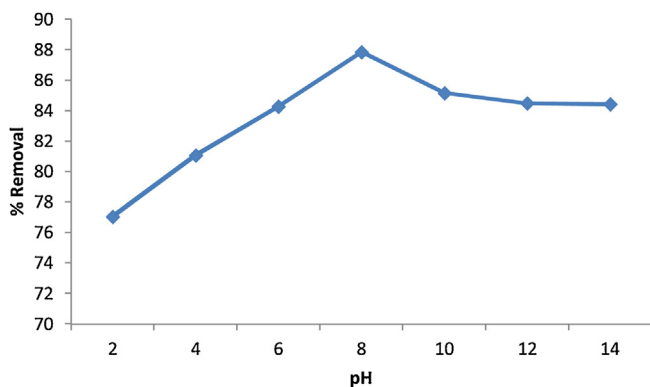


Fig. 6. Effect of pH on lead removal using nanoadsorbent of *Oryza sativa* husk.

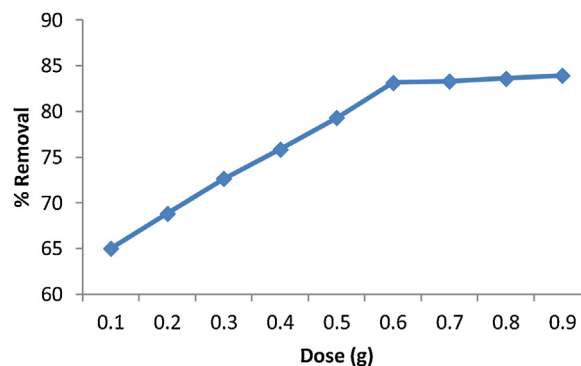


Fig. 7. Effect of dose on lead removal using nanoadsorbent of *Oryza sativa* husk.

and metallic cations that promotes binding of metal ions [1]. At pH 8, precipitation of metal ions occur in the form of hydroxides (as $\text{Pb}(\text{OH})_2$ in the present study). Removal of Pb (II) is affected more by precipitation than adsorption. It is supported by the fact that van der Waals forces of attraction tends to increase Pb (II) binding onto nanocellulose when precipitation occurs. Therefore, pH 8 was set for further experiments.

3.2.2. Effect of adsorbent dose on Pb (II) removal

The influence of dose on Pb (II) removal was carried out in the range of 0.1 g–0.9 g/50 mL keeping other experimental parameters constant. Fig. 7 shows that with increment of nanoadsorbent dose Pb (II) removal raised from 65 % to 83 % and at 0.6 g dose the removal was maximum. It may be due to progressive increase in surface area or availability of exchangeable active sites on the surface of adsorbent that make easy incursion of lead ions to the adsorption sites. At dose 0.6 g, an equilibrium was achieved and on further addition of adsorbent dose percent removal of lead slightly increased. However, adsorption capacity of the adsorbent decreased from 16.26 to 3.46 mg/g when adsorbent dose was

increased as presented in Fig. 7a. It is supported by the fact that the active sites get overlapped on the nanoadsorbent surface due to overcrowding [23].

3.2.3. Effect of contact time on Pb (II) removal

The removal efficiency of nanoadsorbent used is affected by contact time parameter because of equilibrium nature of Pb (II) removal. Therefore, the effect of time on the removal of Pb (II) by nanoadsorbent was analyzed in batch mode. It can be ascertained from the Fig. 8 that Pb (II) removal increased from 69% to 84% with increase in contact time from 10 min to 70 min and arrived at nearly constant amount at equilibrium conditions after 70 min. This sorption variation may be due to relatively high concentration gradient and vacant surface active sites in the beginning [37]. Later on at 70 min the surface active sites get saturated with lead metal ions and almost constant removal efficiency was acquired [24].

3.2.4. Effect of metal ion concentration on Pb (II) removal

The concentration of Pb (II) was varied in the range 10 mg/L to 100 mg/L to study its effect in batch mode. Fig. 9 depicts the

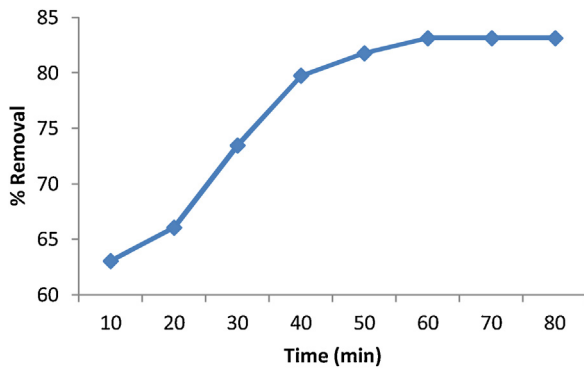


Fig. 8. Effect of time on lead removal using nanoadsorbent of *Oryza sativa* husk.

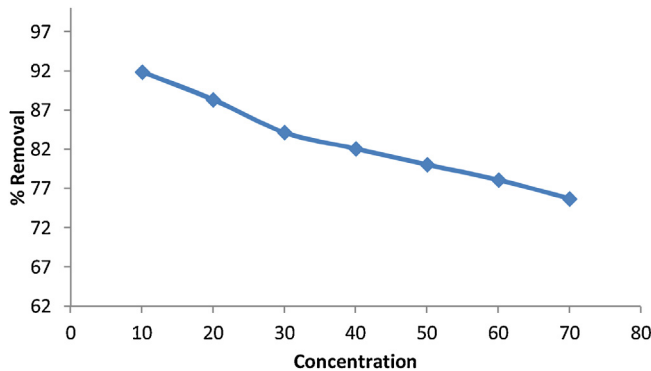


Fig. 9. Effect of concentration on lead removal using nanoadsorbent of *Oryza sativa* husk.

decrease in Pb (II) removal from 91.9 %–75.74 % when initial metal ion concentration was raised. At lower concentration i.e. 10 mg/L, maximal Pb (II) removal was due to availability of many active sites on the surface of nanoadsorbent. However, with increase in concentration surface active sites got saturated with metal ions and resulted in decreased removal of Pb (II). Similar results were given by [21]. Contrarily adsorption capacity increased from 0.75 to 4.41 mg/g with increase in metal ion concentration presented in Fig. 9a. This can be ascribed to upraised mass transfer rate owing to strengthening of driving force [25].

3.2.5. Effect of temperature on Pb (II) removal

The effect of temperature on Pb (II) removal was investigated with 10 °C–60 °C temperature range for 60 min at pH 8 with 0.6 g adsorbent dose. As the temperature increased the Pb (II) removal increased from 81 % to 91 % as depicted in Fig. 10 indicating the process to be endothermic in nature. Pb (II) removal pertains to physical as well as chemical sorption. This may be due to busting of internal bonds at higher temperature resulting in increased active sites at the nanoadsorbent surface. Similar trends were observed by [26].

3.3. Adsorption experiments study

The experimental data for lead metal uptake and heterogeneity or homogeneity of adsorbent was justified by adsorption isotherm models including Langmuir [27], Freundlich [28] and Temkin [29]. Representation of models in linear form is given by Eqs. (3)–(5) respectively.

$$\frac{C_e}{q_e} = \frac{1}{q_{\max} b} + \frac{C_e}{q_{\max}} \quad (3)$$

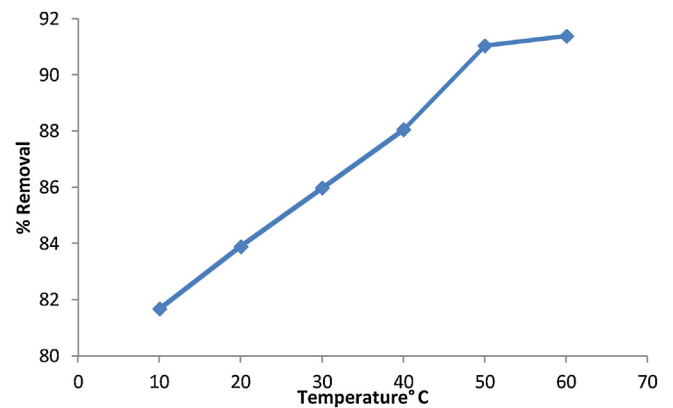


Fig. 10. Effect of temperature on lead removal using nanoadsorbent of *Oryza sativa* husk.

$$\log q_e = \log K_f + \frac{1}{n} \log C_e \quad (4)$$

$$q_e = B \ln K_T + B \ln C_e \quad (5)$$

Where q_{\max} (mg/g) is maximum monolayer adsorption capacity, b (L/mg) is Langmuir constant. The linear plot was derived between C_e/q_e versus C_e to calculate adsorption parameters. K_f (mg/g (L/mg)^{1/n}) is Freundlich constant associated with adsorption capacity and n is heterogeneity factor. The K_f and n values were calculated from the linear plot drawn between $\log q_e$ versus $\log C_e$. The n value should lie between 1 and 10 for favourable adsorption. $\ln B = RT/b$, b (J mol⁻¹) is Temkin constant related to heat of adsorption and K_T (Lg⁻¹) is equilibrium binding constant. The values of K_T and B were calculated by graph between q_e and $\ln C_e$. The values of adsorption parameters and correlation coefficient are given in Table 1.

Comparative correlation coefficient (R^2) values 0.999, 0.9576 and 0.934 of Freundlich, Langmuir and Temkin models respectively indicate fitness of the adsorption data. However, higher value of correlation coefficient R^2 0.999 of Freundlich model in comparison to other studied models is correlative of the multilayer distribution of lead on heterogeneous active sites present on the nanoadsorbent. R^2 value greater than 0.980 and higher than 1.0 n value expressed favorable adsorption. The Langmuir model with 6.101 mg/g adsorption capacity exhibits monolayer adsorption on homogeneous active sites of nano-adsorbent. This contributes to the fact that the said nano-adsorbent has a high surface area specifically in nano proportions [24].

The adsorption capacity of Pb (II) was compared with different studied nanocellulose adsorbents and encapsulated in Table 1.

Table 1

Comparative study of adsorption capacity of different adsorbents for Pb (II) removal.

Adsorbent	qmax	References
Rice straw nanocellulose	10.20 mg/g	[30]
Wheat pulp nanocellulose	1.2 m mol/g	[31]
Clinoptilolite nanoparticles NCP	0.283 m mol/g	[32]
NCP-DTZ	0.275 m mol/g	[32]
NCP-Pb-HDTMA-DTZ	0.393 m mol/g	[32]
Rice husk nanoadsorbent	6.101 mg/g	Present study

Table 2
Thermodynamic parameters for adsorption of lead onto nanocellulose.

Temp. (K)	ΔG (kJ mol ⁻¹)	ΔS (J mol ⁻¹ K ⁻¹)	ΔH (kJ mol ⁻¹)
283	-12.19	43.14	14.634
293	-12.62		
303	-13.06		
313	-13.48		
323	-13.92		
333	-14.35		

Table 3
Parameters for lead adsorption onto nanocellulose through Kinetic models.

Kinetic model	Parameters	Values
Pseudo-first order	q_e (mg/g) (cal)	2.2187
	k_1 (min ⁻¹)	0.0683
	R^2	0.9311
Pseudo-second order	q_e (mg/g) (cal)	3.783
	k_2 (g/mg min)	0.048
	R^2	0.996
Intraparticle diffusion	k_{id} (mg/g/min ⁻¹)	0.1586
	C_T	2.18
	R^2	0.906

3.4. Thermodynamic study

Thermodynamic parameters viz. (i) Gibb's free energy (ΔG°), (ii) enthalpy (ΔH°) and (iii) entropy (ΔS°) were calculated using equilibrium constant varying with temperature. The Gibb's free energy was given by Vent Hoff's equation

$$\Delta G^\circ = -RT \ln K_d \quad (6)$$

$$K_d = \frac{C_a(\text{Amount of Pb (II) in adsorbent})}{C_e(\text{Amount of Pb (II) in solution})} \quad (7)$$

Where R (8.314 J mol⁻¹ K⁻¹) is gas constant, K_d is equilibrium constant and T (K) is temperature. The change in Gibb's free energy, enthalpy and entropy is represented by following equations:

$$\Delta G^\circ = \Delta H^\circ - T \Delta S^\circ \quad (8)$$

$$\ln K_d = \frac{\Delta S^\circ}{2.303R} + \frac{-\Delta H^\circ}{2.303RT} \quad (9)$$

Where ΔS° is entropy and ΔH° is enthalpy. The values of ΔH° and ΔS° are given by slope and intercept obtained from plot between $\ln K_d$ vs $1/T$. The positive value of ΔH° 14.634 kJ mol⁻¹ indicates endothermic nature of the lead adsorption process presented in Table 2. The positive value of ΔS° 43.14 kJ mol⁻¹ account for increased randomness during lead adsorption. The negative value of ΔG° -12.193 kJ mol⁻¹ confirms feasibility and spontaneity of adsorption process. Chemical sorption was confirmed by negative values of Gibb's free energy and supported by [33].

3.5. Kinetic study

Transport rate mechanism of adsorbate in adsorbent was provided by kinetic data. Langergran's pseudo first order [34] and Ho's pseudo second order [35] kinetic equations were used to describe kinetics of Pb (II) on to OSH nanoadsorbent.

$$\log q_e - q_t = \log q_e - \left(\frac{k_1}{2.303} \right) t \quad (10)$$

$$\frac{t}{qt} = \frac{1}{k_2 q_e^2} + \frac{t}{q_e} \quad (11)$$

where k_1 (min⁻¹) is pseudo first-order rate constant and k_2 (mg/g min⁻¹) is pseudo second-order rate constant in adsorption kinetics, q_e (mg/g) and q_t (mg/g) are adsorption capacities per unit weight at equilibrium and at any time t . Eq. (10) can be drawn from $\log(q_e - q_t)$ vs t plots gives k_1 and q_e values. Eq. (11) can be drawn by Slope and intercept of the plot gives values of k_2 and q_e . Experimental data for both the kinetic models represent high correlation coefficients.

Comparing the values of correlation coefficient for both the models indicate that R^2 (0.996) for pseudo second-order is higher than R^2 (0.9311) of pseudo first-order as depicted in Table 3. It is indicative of better fit of Pb (II) adsorption data into pseudo second-order kinetics. Further Pb (II) removal results indicate that adsorption may be rate limiting step that possess valence forces among adsorbent and sorbate with exchange or share of electrons [36].

3.6. Adsorption mechanism

Adsorption mechanism of metal ions depends on various factors viz. pH of the solution, metals chemistry in solution, binding characteristics. Usually metal ion adsorption is

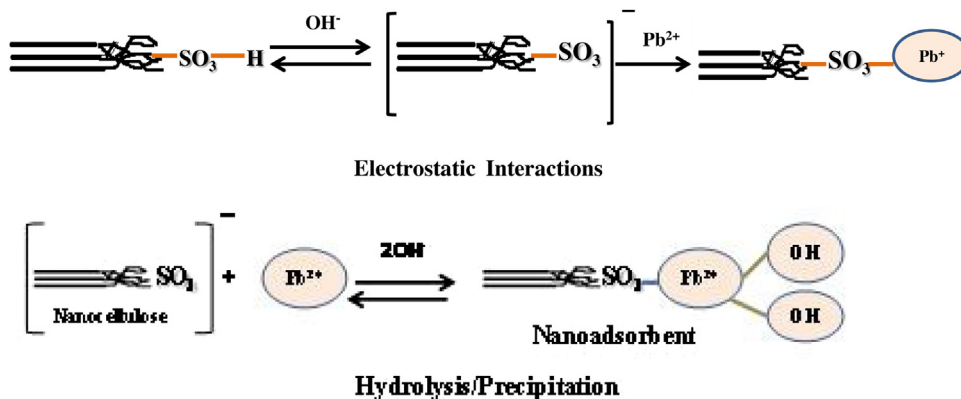


Fig. 11. Schematic mechanism of lead interaction with OSH nanoadsorbent.

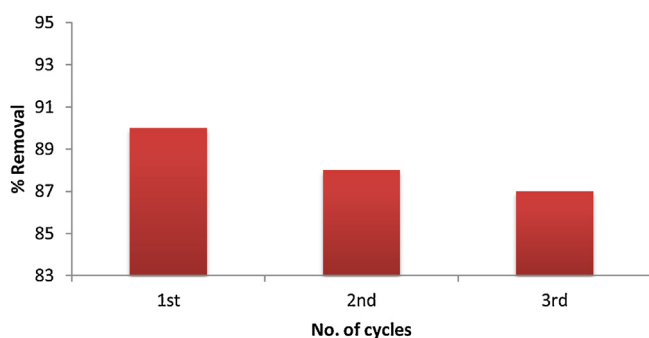


Fig. 12. Reusability of nanoadsorbent for lead from aqueous solution.

accomplished by ion exchange, complex formation, electrostatic interaction and precipitation. In present study, Pb (II) adsorption is explained by pH effect and characterization techniques viz. FTIR, FESEM and EDX which supported the binding of metals on OSH nanoadsorbent as oxides and hydroxides. These groups electrostatically interact with Pb^{2+} and $Pb(OH)^+$ and at higher pH lead hydroxides get precipitated on the surface of OSH nanoadsorbent. Fig. 11(a&b) illustrated the adsorption of lead ions onto the surface of OSH nanoadsorbent.

3.7. Reusability efficiency

The reusable demonstration of adsorbent is very important for sustainability and economic point of view. The reusability of nanoadsorbent OSH for Pb (II) was investigated upto three successive cycles with 0.1 M HCl. The Pb (II) adsorption was observed after the addition of 0.6 g nanoadsorbent in 50 mL metal ion solution keeping 8 pH, 10 mg/L metal ion concentration and 60 min time constant. The spent adsorbent was separated from the solution after adsorption and washed with distilled water. At 80 °C temperature the spent adsorbent was dried for 3 h and used further for Pb (II) adsorption. The removal efficiency of nanoadsorbent for Pb (II) decreased to 87 % after third cycle as depicted in Fig. 12. It may be due to the loss of surface active sites during adsorption-desorption process.

3.8. Conclusion

The present study concluded as: (i) nanoadsorbent from OSH (*Oryza sativa* husk, an abundantly available agricultural waste) synthesized by chemo-mechanical method is efficacious for removal of lead from aqueous solution. (ii) The surface morphology and size of nanocellulose was measured by FE-SEM and AFM and adsorption of lead onto nanocellulose and elemental composition were confirmed by FESEM and EDX. (iii) Pb (II) adsorption is pH, adsorbent dose and temperature dependent. (iv) Equilibrium data with Freundlich isotherm model is best fitted to Pb (II) adsorption with R^2 0.9991 supporting the multilayer adsorption. (v) Rate transport mechanism is in good agreement with Pseudo-second order having genuine correlation and adsorption capacity 3.783 mg/g. (vi) Spontaneous nature and feasibility of Pb (II) adsorption process was confirmed by thermodynamic studies. (vii) These results incited OSH nanoadsorbent to be economically executable for Pb (II) removal from aqueous solution.

CRedit authorship contribution statement

Mandeep Kaur: Conceptualization, Methodology, Data curation, Writing - original draft. **Santosh Kumari:** Visualization,

Investigation. **Praveen Sharma:** Supervision, Validation, Investigation.

Declaration of competing interest

The authors declare that they have no conflict of interest.

Acknowledgements

We gratefully acknowledge the UGC-BSR fellowship (grant/letter no. 25-1/2013-14/BSR), CIRCOT-Mumbai for AFM, Central University Bathinda for FE-SEM and EDX.

References

- [1] M. Kaur, P. Sharma, S. Kumari, et al., Equilibrium studies for copper removal from aqueous solution using nanoadsorbent synthesized from rice husk, *SN Appl. Sci.* 1 (2019) 1–9.
- [2] Z. Kariuki, J. Kiptoo, D. Onyancha, et al., Biosorption studies of lead and copper using rogers mushroom biomass 'Lepiota hystrix', *S. Afr. J. Chem. Eng.* 23 (2017) 62–70.
- [3] P.J. Harvey, H.K. Handley, M.P. Taylor, et al., Identification of the sources of metal (lead) contamination in drinking waters in north-eastern Tasmania using lead isotopic compositions, *Environ. Sci. Pollut. Res.* 22 (2015) 12276–12288.
- [4] J.R.M.B. Smily, P.A. Sumithra, Optimization of chromium biosorption by fungal adsorbent, *Trichoderma* sp. BSCR02 and its desorption studies, *HAYATI J. Biosci.* 24 (2) (2017) 65–71.
- [5] R. Saravanan, V.K. Gupta, V. Narayanan, A. Stephen, et al., Visible light degradation of textile effluent using novel catalyst ZnO/ γ -Mn₂O₃, *J. Taiwan Inst. Chem. Eng.* 45 (2014) 1910–1917.
- [6] A.N. Amro, M.K. Abhary, et al., Removal of lead and copper ions from water using powdered *Zygothphyllum coccineum* biomass, *Int. J. Phytorem.* 6 (2019) 1–6.
- [7] S. Uçar, M. Erdem, T. Tay, S. Karagöz, et al., Removal of lead (II) and nickel (II) ions from aqueous solution using activated carbon prepared from rapeseed oil cake by Na₂CO₃ activation, *Clean Technol. Environ. Policy* 17 (2015) 747–756.
- [8] X. Qu, P.J. Alvarez, Q. Li, et al., Applications of nanotechnology in water and wastewater treatment, *Water Res.* 47 (2013) 3931–3946.
- [9] N. Kataria, V.K. Garg, Optimization of Pb (II) and Cd (II) adsorption onto ZnO nanoflowers using central composite design: isotherms and kinetics modelling, *J. Mol. Liq.* 271 (2018) 228–239.
- [10] Y. Ku, I.L. Jung, Photocatalytic reduction of Cr (VI) in aqueous solutions by UV irradiation with the presence of titanium dioxide, *Water Res.* 35 (2001) 135–142.
- [11] N. Dizge, B. Keskinler, H. Barlas, et al., Sorption of Ni (II) ions from aqueous solution by Lewatit cation-exchange resin, *J. Hazard. Mater.* 167 (2009) 915–926.
- [12] K. Trivunac, S. Stevanovic, Removal of heavy metal ions from water by complexation-assisted ultrafiltration, *Chemosphere* 64 (2006) 486–491.
- [13] L.H. Andrade, A.O. Aguiar, W.L. Pires, G.A. Miranda, L.P.T. Teixeira, G.C.C. Almeida, M.C.S. Amaral, et al., Nanofiltration and reverse osmosis applied to gold mining effluent treatment and reuse, *Braz. J. Chem. Eng.* 34 (2017) 93–107.
- [14] M. Ahmaruzzaman, V.K. Gupta, et al., Rice husk and its ash as low-cost adsorbents in water and wastewater treatment, *Ind. Eng. Chem. Res.* 50 (2011) 13589–13613.
- [15] H. Guo, S. Zhang, Z. Kou, S. Zhai, W. Ma, Y. Yang, et al., Removal of cadmium (II) from aqueous solutions by chemically modified maize straw, *Carbohydr. Polym.* 115 (2015) 177–185.
- [16] A.E. Burakov, E.V. Galunin, I.V. Burakova, A.E. Kucherova, S. Agarwal, A.G. Tkachev, V.K. Gupta, et al., Adsorption of heavy metals on conventional and nanostructured materials for wastewater treatment purposes: a review, *Ecotoxicol. Environ. Saf.* 148 (2018) 702–712.
- [17] M. Kaur, P. Sharma, S. Kumari, et al., Extraction preparation and characterization: nanocellulose, *Int. J. Sci. Res.* 6 (2017) 1881–1886.
- [18] M. Ghaedi, S. Hajjati, Z. Mahmudi, I. Tyagi, S. Agarwal, A. Maity, V.K. Gupta, et al., Modeling of competitive ultrasonic assisted removal of the dyes—methylene blue and Safranin-O using Fe₃O₄ nanoparticles, *Chem. Eng. J.* 268 (2015) 28–37.
- [19] M. Kaur, S. Kumari, P. Sharma, et al., Chemically modified nanocellulose from rice husk: synthesis and characterisation, *Adv. Res.* 13 (2018) 1–11.
- [20] M.M. Haafiz, S.J. Eichhorn, A. Hassan, M. Jawaid, Isolation and characterization of microcrystalline cellulose from oil palm biomass residue, *Carbohydr. Polym.* 93 (2013) 628–634.
- [21] N. Li, L. Zhang, Y. Chen, Y. Tian, H. Wang, et al., Adsorption behavior of Cu (II) onto titanate nanofibers prepared by alkali treatment, *J. Hazard. Mater.* 189 (2011) 265–272.
- [22] E. Demirbas, N. Dizge, M.T. Sulak, M. Kobya, et al., Adsorption kinetics and equilibrium of copper from aqueous solutions using hazelnut shell activated carbon, *Chem. Eng. J.* 148 (2009) 480–487.

- [23] S.M. Ghasemi, A.N. Mohseni-Bandpei, M. Ghaderpoori, Y.A. Fakhri, H.A. Keramati, M. Taghavi, B.I. Moradi, K. Karimyan, et al., Application of modified maize hull for removal of Cu (II) ions from aqueous solutions, *Process Saf. Environ. Prot.* 43 (2017) 93–103.
- [24] A. Nezamzadeh-Ejhieh, M. Kabiri-Samani, Effective removal of Ni (II) from aqueous solutions by modification of nano particles of clinoptilolite with dimethylglyoxime, *J. Hazard. Mater.* 260 (2013) 339–349.
- [25] U.K. Garg, M.P. Kaur, V.K. Garg, D. Sud, et al., Removal of nickel (II) from aqueous solution by adsorption on agricultural waste biomass using a response surface methodological approach, *Bioresour. Technol. Rep.* 99 (2008) 1325–1331.
- [26] T. Fan, Y. Liu, B. Feng, G. Zeng, C. Yang, M. Zhou, X. Wang, et al., Biosorption of cadmium (II), zinc (II) and lead (II) by *Penicillium simplicissimum*: isotherms, kinetics and thermodynamics, *J. Hazard. Mater.* 160 (2008) 655–661.
- [27] I. Langmuir, The constitution and fundamental properties of solids and liquid, *J. Am. Soc. Brew. Chem.* 38 (1916) 2221–2295.
- [28] H.M.F. Freundlich, Over the adsorption in solution, *J. Phys. Chem.* 57 (1906) 385–471.
- [29] M.J. Temkin, V. Pyzhev, Recent modifications to Langmuir isotherms, *Acta Phys. Chim.* 12 (1940) 217–222.
- [30] A. Kardam, K.R. Raj, S. Srivastava, M.M. Srivastava, et al., Nanocellulose fibers for biosorption of cadmium, nickel, and lead ions from aqueous solution, *Clean Technol. Environ. Policy* 16 (2014) 385–393.
- [31] T. Suopajärvi, H. Liimatainen, M. Karjalainen, H. Upola, J. Niinimäki, et al., Lead adsorption with sulfonated wheat pulp nanocelluloses, *J. Water Process. Eng.* 5 (2015) 136–142.
- [32] M. Anari-Anaraki, A. Nezamzadeh-Ejhieh, Modification of clinoptilolite nanoparticles by a cationic surfactant and dithizone for removal of Pb (II) from aqueous solution, *J. Colloid Interface Sci.* 440 (2015) 272–281.
- [33] M. Borandegi, A. Nezamzadeh-Ejhieh, Enhanced removal efficiency of clinoptilolite nano-particles toward Co (II) from aqueous solution by modification with glutamic acid, *Colloids Surf. A: Physicochem. Eng. Asp.* 479 (2015) 35–45.
- [34] S. Lagergren, Zur theorie der sogenannten adsorption gelöster stoffe, *Kung Sven Vetén Hand* 24 (1898) 1–39.
- [35] Y.S. Ho, J.C.Y. Ng, G. McKay, et al., Kinetics of pollutant sorption by biosorbents, *Sep. Purif. Method* 29 (2000) 189–232.
- [36] M.A. Shavandi, Z. Haddadian, M.H.S. Ismail, N. Abdullah, Z.Z. Abidin, et al., Removal of Fe (III), Mn (II) and Zn (II) from palm oil mill effluent (POME) by natural zeolite, *J. Taiwan Chem. Eng.* 43 (2012) 750–759.
- [37] M.M. Ibrahim, W.W. Ngah, M.S. Norliyana, W.W. Daud, M. Rafatullah, O. Sulaiman, R. Hashim, A novel agricultural waste adsorbent for the removal of lead (II) ions from aqueous solutions, *J. Hazard. Mater.* 182 (2010) 377–385.
- [38] S.N. Farhan, A.A. Khadom, Biosorption of heavy metals from aqueous solutions by *Saccharomyces Cerevisiae*, *Int. J. Ind. Chem.* 6 (2) (2015) 119–130.